

# The effect of pressure on the structural and electronic properties of yttrium orthovanadate $\text{YVO}_4$ compound: total-energy calculations

Messekine Souad<sup>I,III</sup>, Sahnoun Mohammed<sup>\*,I</sup>, Driz Mohamed<sup>II</sup> and Daul Claude<sup>III</sup>

<sup>I</sup> Laboratoire de Physique Quantique de la Matière et de Modélisation Mathématiques (LPQ3M). Université de Mascara. B.P 763 Mascara, Algeria

<sup>II</sup> Applied Materials Laboratory (AML), Université de Sidi-bel-Abbes, 22000, Algeria

<sup>III</sup> Département de Chimie, Université de Fribourg, Chemin du Musée 9, 1700 Fribourg, Switzerland

Received July 31, 2010; accepted September 22, 2010

*Ab-initio calculations / Structural phase transition / Electronic properties / Pressure effect*

**Abstract.** We have investigated the structural properties and electronic properties of the zircon-type and the scheelite-type  $\text{YVO}_4$  using first-principles method and by considering Engel-Vosko exchange correlation energy functional. The calculated lattice parameters and the atomic positions of the zircon-type  $\text{YVO}_4$  are in good agreement with the experiment. We also found from this study that  $\text{YVO}_4$  is stable in the zircon-type, and the calculated phase transition pressure from the zircon-type structure to the scheelite-type structure is about 5.92 GPa, which compares well with the experimental value of 7.5 GPa. From the density of states and band structures, the linearized augmented plane wave (LAPW) calculations indicate that the minimum band gap of  $\text{YVO}_4$  is located at the  $\Gamma$  point at the center of the Brillouin zone, for both phases. The calculated band gaps are 3.2 eV and 2.8 eV for the zircon-type phase and the scheelite-type phase, respectively.

## Introduction

A great progress has been done in the last years in the study of the pressure-effects on the structural and electronic properties of materials, including metals, semiconductors, superconductors, or minerals. In particular, the high-pressure structural sequence followed by these compounds seems now to be better understood thanks to recent experimental and theoretical studies. An accurate first-principles method of calculating the structural properties of such materials are, therefore, very valuable. Such calculations can also predict pressure-induced phase transitions. Theoretical studies of such phase transitions have been of special interest over the last three decades. Compounds of the family  $\text{ABX}_4$  are widely used as solid state scintillator materials, laser host materials, in opto-electronic devices, etc. So there is a renewed interest in the study of the phase transition behavior of these systems. Among the exten-

sively investigated systems of this family are orthovanadates [1], and most of these compounds crystallize either in the zircon-type [space group  $I4_1/amd$ ,  $Z = 4$ ] or the scheelite-type structure [space group  $I4_1/a$ ,  $Z = 4$ ] at ambient conditions. Yttrium orthovanadate  $\text{YVO}_4$  crystallizes in the zircon-type structure at ambient conditions. The compound is attractive for technological applications owing to its properties such as large refractive indices, non-linear coefficients, birefringence and effectively no infrared absorption from 2.5 to 15  $\mu\text{m}$  [2]. Yttrium orthovanadate  $\text{YVO}_4$  can be considered as the oldest laser host crystal for  $\text{Nd}^{3+}$  ions [3–5], as well as being a highly efficient red-emitting phosphor when doped with  $\text{Eu}^{3+}$  [6]. Due to its high birefringence,  $\text{YVO}_4$  is an excellent synthetic substitute for calcite ( $\text{CaCO}_3$ ), and can provide crystalline polarizers for the mid-infrared (as Wollaston, Rochon, and Glan prisms) [7]. In the last decade,  $\text{Nd}^{3+}$ -doped  $\text{YVO}_4$  has been successfully used in laser-diode pumped micro-lasers (see, for example, Refs. [8–10]). The high pressure properties of similar compounds are interesting since at moderate pressures (8 GPa) the zircon-type structure transforms to a denser scheelite-type phase [1, 11–14], irreversibly whereas at lower temperatures 40 K some of orthovanadate family members transform to a lower symmetry structure via a cooperative Jahn–Teller transition [19]. The pressure dependences of the Raman active modes in yttrium orthovanadate  $\text{YVO}_4$  crystallizing in the zircon-type structure ( $I4_1/amd$ ), have been studied by Jayaraman *et al.* [1] using a diamond anvil cell up to 15 GPa where they have shown that at room temperature the zircon-type structure transforms to the scheelite-type structure ( $I4_1/a$ ) with  $a = 5.04 \text{ \AA}$  and  $c = 11.24 \text{ \AA}$  near 7.5 GPa. The electronic structures of the zircon polymorph of  $\text{YVO}_4$  have previously been reported both experimentally and computationally [20, 21]. They were interpreted from the  $\text{VO}_4^{3-}$  molecular orbital diagram as the  $\text{Y}^{3+}$  cations make a negligible contribution to the electronic structure near the Fermi level. In contrast, the  $\text{Y}^{3+}$  cation orbitals have a considerable impact on the positions of the valence and conduction band edges in this compound. Mechanical properties have also been calculated and reported by Jian Zhang *et al.* [15].

\* Correspondence author (e-mail: sahnoun\_cum@yahoo.fr)

However detailed characteristic of YVO<sub>4</sub> have not been well investigated. We therefore think that it is worthwhile to perform calculations using the full-potential linearized augmented plane wave method (FP-LAPW) method in order to complete the exciting experimental and theoretical works on this compound.

## Computational details

The equilibrium structure, phase transition pressure and electronic properties of YVO<sub>4</sub> were determined using the Vienna package Wien2k [20]. This is a full-potential linearized augmented plane waves (FP-LAPW) method within the density functional theory (DFT) [21]. We used the generalized gradient approximation (GGA) proposed by Engel and Vosko (GGA-EV) [22] which has been designed to give a better exchange correlation potential and it is known to yield the smallest band gap underestimation error in DFT. Relativistic effects are taken into account via the scalar approximation. Muffin-tin (MT) sphere radii of 2.17, 1.61 and 1.43 Bohr were used for Y, V and O atoms, respectively. The valence wave functions inside the MT spheres were expanded into spherical harmonics up to  $l = 10$  and  $R_{mt} \cdot K_{max}$  were taken to be 8.0. We used 1000  $k$ -points in the Brillouin zone for the zircon-type structure and 1300  $k$ -points for the scheelite-type structure. The self-consistent calculations were considered to be converged only when the total energy cycles converge to within 0.1 mRy/atom.

## Results and discussion

### Structural properties and phase transition

The conventional unit cells of the zircon-type (space group  $I4_1/amd$ , No. 141) and the scheelite-type (space group  $I4_1/a$ , No. 88) structures are body-centered tetragonal and contain four formula units. A primitive cell containing only two formula units can be defined. In order to illustrate the relative arrangement of cations unambiguously, we choose V positions as the origins of the unit cells, as shown in Fig. 1. In both structures, the V ions are tetrahedrally coordinated by O ions, but with different interatomic distances and angles. In the zircon-type structure, the Y and V atoms are located at  $(0, \frac{3}{4}, \frac{1}{8})$  and  $(0, \frac{1}{4}, \frac{3}{8})$  on the  $4a$  and  $4b$  Wyckoff sites, respectively. The O atoms occupy the  $16h$  Wyckoff sites  $(0, y_1, z_1)$ , where  $y_1$  and  $z_1$  are internal parameters. In the scheelite-type structure, Y and V atoms are located at  $(0, \frac{1}{4}, \frac{5}{8})$  and  $(0, \frac{1}{4}, \frac{1}{8})$  on the  $4b$  and  $4a$  Wyckoff sites, respectively. The O atoms occupy the  $16f$  Wyckoff sites  $(x_2, y_2, z_2)$ , where  $x_2, y_2$  and  $z_2$  are internal parameters. The zero-pressure structural parameters of the zircon-type and the scheelite-type YVO<sub>4</sub> are summarized in Table 1. The lattice parameters and the oxygen positions of the scheelite-type phase are calculated for the first time. For the zircon-type phase, our calculated lattice parameters are in excellent agreement to the experimental results of Wang *et al.* [23]. We obtain good lattice parameters, however the bulk moduli are larger than the measured ones. The bulk modulus

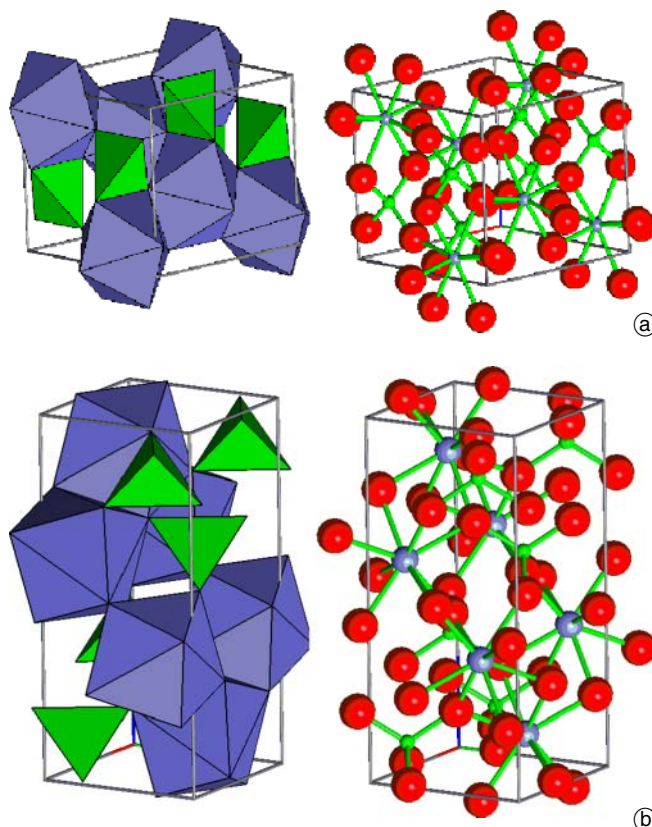


**Fig. 1.** Crystal structure of yttrium orthovanadate (YVO<sub>4</sub>), in the (a) zircon-type and (b) scheelite-type structures: Y, the small blue balls; V, small green balls; O, large red balls.

(B) was evaluated from the Birch-Murnaghan equation fit to determine the equation-of-state (EOS) which determines the variation of total energies as a function of the unit cell volume.

$$E(V) = E_0 + \frac{9V_0B}{16} \left\{ \left[ \left( \frac{V_0}{V} \right)^{\frac{2}{3}} - 1 \right]^3 B' + \left[ \left( \frac{V_0}{V} \right)^{\frac{2}{3}} - 1 \right]^2 \left[ 6 - 4 \left( \frac{V_0}{V} \right)^{\frac{2}{3}} \right] \right\} \quad (1)$$

The calculated bulk modulus is  $B = 164$  GPa for the zircon-type phase and  $B = 186$  GPa for the scheelite-type phase. The scheelite-type phase bulk modulus is larger than that of the zircon-type phase and it reveals that the scheelite-type phase is more difficult to compress than the zircon-type phase. This is reasonable since the scheelite-type phase is the high-pressure phase which is more closely packed than the zircon-type phase. In the Fig. 2 the intersection of convex curves representing EOS fit of the scheelite-type and the zircon-type implies that the phase transition exists.

By calculating the enthalpy ( $E + PV$ ) of the phases, we find the pressure at which a first-order phase transition occurs at  $T = 0$  K. At transition pressure, the enthalpies for two phases are equal and a stable structure is the one for which the enthalpy has the lowest value. We find that the calculated transition pressure from the zircon-type phase to the scheelite-type phase occurs at 5.92 GPa, which compares well with the experimental value (7.5 GPa) reported

Structure type		Zircon-type phase	Scheelite-type phase
Space Group		$I4_1/amd$	$I4_1/a$
Lattice parameters	$a, b$ (Å)	7.110	5.070
		7.179 <sup>18</sup>	5.080 <sup>24</sup>
	Exp.	7.122 <sup>23</sup>	5.032 <sup>23</sup>
		$c$ (Å)	6.280
	Exp.	6.313 <sup>18</sup>	11.348 <sup>24</sup>
		6.291 <sup>23</sup>	11.233 <sup>23</sup>
Bulk modulus	$B$ (GPa)	164.578	186.748
		Exp.	123.300 <sup>24</sup>
	$B'$	4.107	4.224
		5.400 <sup>24</sup>	3.800 <sup>24</sup>
	Exp.	4.400 <sup>23</sup>	4.500 <sup>23</sup>
Atomic positions	Y	$(0; \frac{3}{4}; \frac{1}{8})$	$(0; \frac{1}{4}; \frac{5}{8})$
	V	$(0; \frac{1}{4}; \frac{3}{8})$	$(0; \frac{1}{4}; \frac{1}{8})$
	O	$(0.0; 0.43510; 0.20280)$	$(0.25450; 0.15050; 0.04441)$
Interatomic distances	Y–O (Å)	2.292	2.338
		2.443	2.549
		3.140	3.585
	Y–V (Å)	3.140	3.585
		V–O (Å)	1.703
	Angles (°)	O–V–O	101.179
			116.955

**Table 1.** The zero-pressure structural parameters of  $YVO_4$  in the zircon-type and the scheelite-type structures.

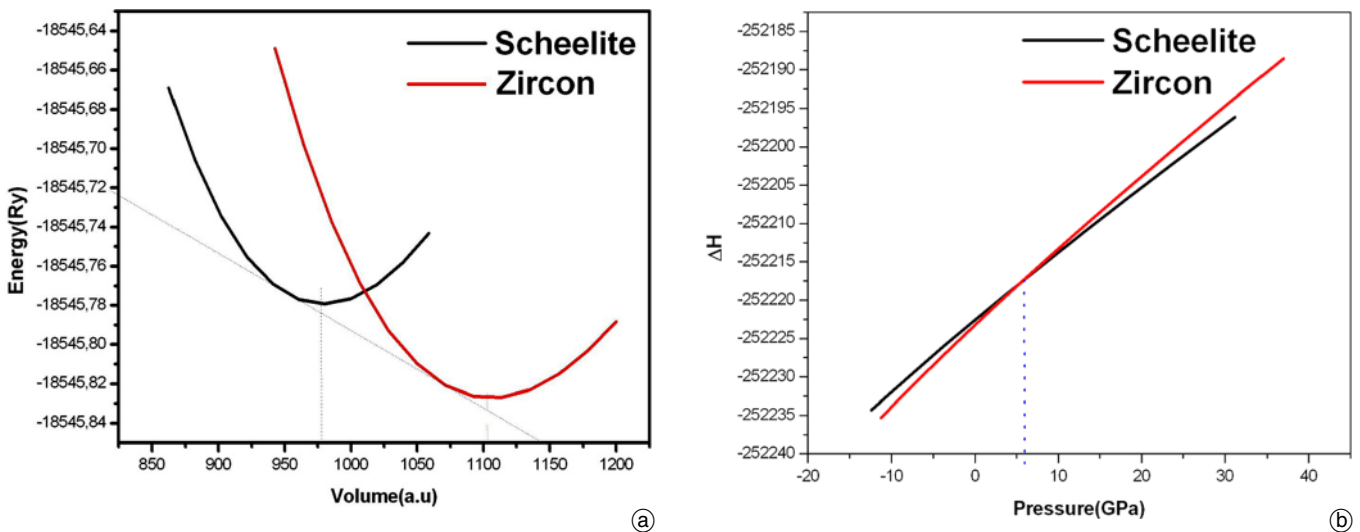


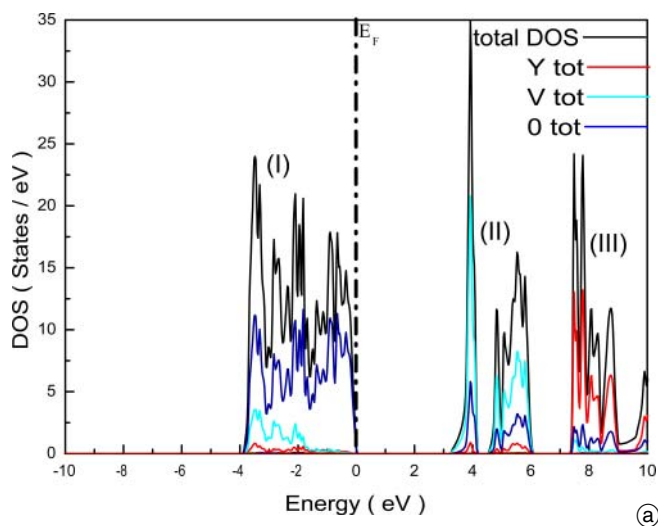
**Fig. 2.** (a) Total energy as a function of unit cell volume for the zircon-type phase and the scheelite-type phase of  $YVO_4$ . (b) Gibbs free energy as a function of pressure.

by Manjon *et al.* [24]. The volume of the zircon-type phase is decreased by 8.49% compared to the scheelite-type one.

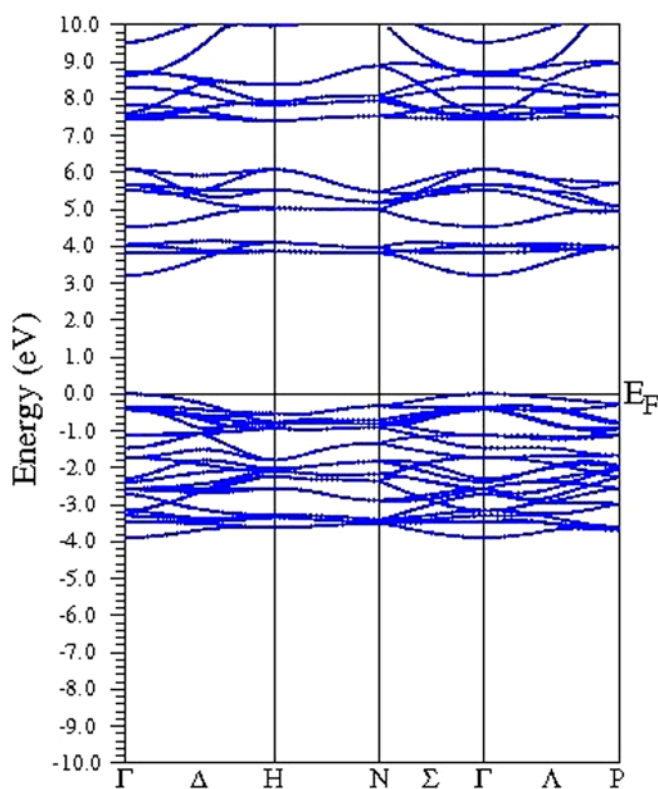
### Density of states (DOS) and band structures

We have calculated the electronic structure of the two phases; the DOS is computed by the tetrahedron method [25] (which requires many  $k$ -points). From the eigenvalues and eigenvectors solved at a sufficient number of  $k$ -points in the Brillouin-zone, the total DOS can be projected into its partial components or partial DOS (PDOS) with respect to the different atoms. In Figs. 3 and 4, we present both the calculated DOS and the bands structures obtained for

the zircon-type and the scheelite-type phases, respectively, of the constituting atoms of  $YVO_4$  within the valence-band and conduction-band regions. The Fermi level corresponding to zero of energy  $E = 0$  has been taken at the top of the last occupied band as it was suggested in a number of theoretical first-principles band-structure calculations. The valence band of  $YVO_4$  ranges from 0 to  $-5$  eV and it is composed mainly from contributions of the valence Y  $4p$ -, Y  $4d$ -, V  $4d$ - and O  $2p$ -like states. The Y  $4p$ -, Y  $4d$ -, and V  $4d$ -like states contribute mainly into the lower portion of the valence band, while the O  $2p$ -like states contribute throughout the valence-band region of  $YVO_4$  with predominant contributions into the bottom and



(a)

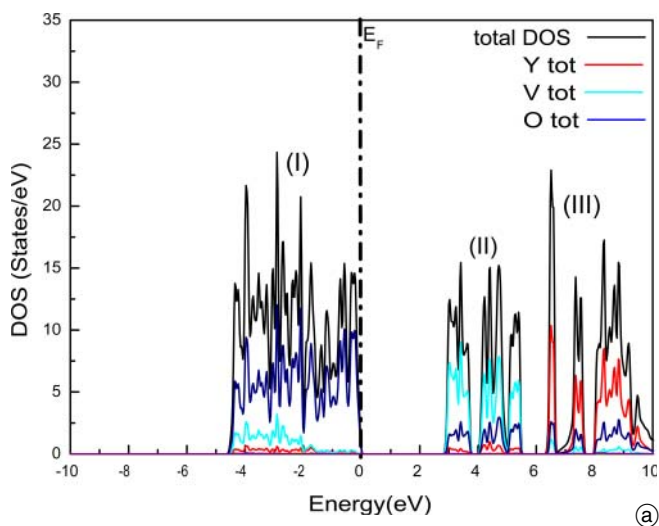


(b)

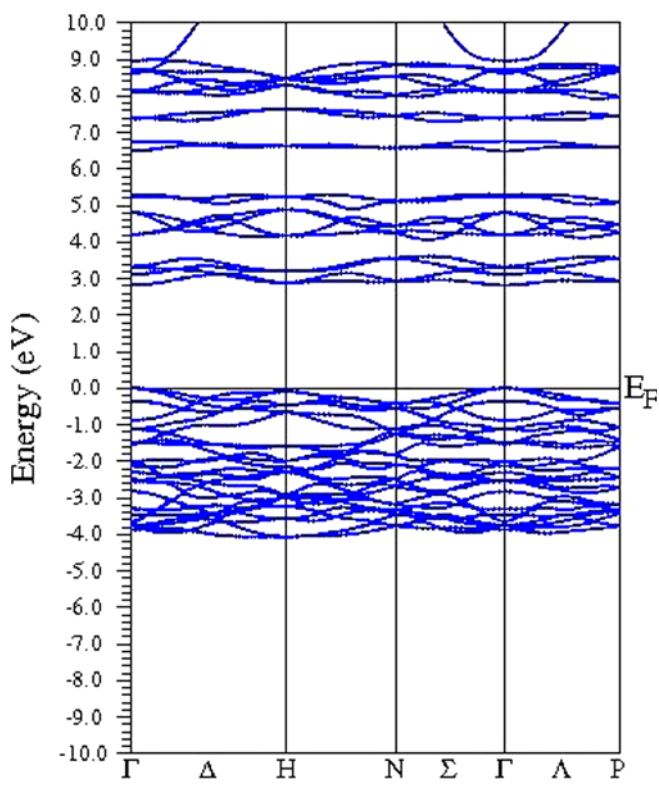
**Fig. 3.** (a) Total and partial density of states and (b) Electronic bands along selected symmetry paths within the first Brillouin zone of YVO<sub>4</sub> in the zircon-type structure (space group  $I4_1/amd$ , No. 141).

the top of the valence band. However, the dominant contributors into the valence-band region of YVO<sub>4</sub> are the O  $2p$ -like states. Further, as mentioned above, the present FP-LAPW calculations predict the increasing width of the valence-band region from 4 to 4.3 eV when going from the zircon-type to the scheelite-type phases of YVO<sub>4</sub>.

Band dispersions for YVO<sub>4</sub> are plotted in Figs. 3(b) and 4(b) for several symmetry directions of the bcc Brillouin zone, which is characteristic of the two phases under consideration. In these figures the coordinates of the  $k$ -points, within the limited region of the Brillouin zone studied for the band dispersions are as follows:  $\Gamma$  (0 0 0),  $H$  (1 0 0),  $N$  ( $1/2$   $1/2$  0),  $\Sigma$  ( $1/4$   $1/4$  0), and  $P$  ( $1/2$   $1/2$   $1/2$ ). YVO<sub>4</sub> is a



(a)



(b)

**Fig. 4.** (a) Total and partial density of states and (b) Electronic bands along selected symmetry paths within the first Brillouin zone of YVO<sub>4</sub> in the scheelite-type structure (space group  $I4_1/a$ , No. 88).

direct-gap material in its both phases; the maximum of the valence band and the minimum of the conduction band are both located at the  $\Gamma$  point in the center of the Brillouin zone. The shapes of the band dispersions for both phases look very similar to each other, as displayed in Figs. 3(b) and 4(b). According to the present FP-LAPW calculations using the Engel-Vosko exchange correlation energy functional [22], the values of the direct gap in YVO<sub>4</sub> equal to 3.2 eV in the zircon-type phase and 2.8 eV in the scheelite-type phase. However, it is necessary to mention that first-principles calculations made within the other GGA approximations generally underestimate somewhat the energy gap of semiconductors and insu-

lators [26]. As a result, we can consider that the value  $E_g = 3.2$  eV obtained theoretically in the present FP-LAPW calculations for  $\text{YVO}_4$  is in good agreement with experimentally measured value  $E_g = 3$  eV reported by Zhi-Peng *et al.* [18] for this material. The first region of the conduction band ranging from 3 to 6 eV and 3 to 5.5 eV for the zircon-type and the scheelite-type  $\text{YVO}_4$ , respectively, is mainly composed of the V  $3d$ -like states with slightly smaller contributions of the O  $2p$ -like states. Significantly smaller contributions of the Y  $4d$ -like states into this region of the conduction band are also detected by the present FP-LAPW calculations. It may be mentioned that the energy gap shift under pressure from 3.2 to 2.8 eV is presumably due to charge transfer from O  $2p$ -like states to V  $3d$ -like states, or due to V–O bond length change of the  $\text{VO}_4$  tetrahedra, which is compressed from 1.703 to 1.658 Å. Figs. 3(a) and 4(a) reveal that the V  $3d$ -, Y  $4d$ - and O  $2p$ -like states are somewhat hybridized within the conduction band of  $\text{YVO}_4$ . Further, one can conclude that contributions of the states, associated with Y, into the first region of the conduction band of  $\text{YVO}_4$  are minor. It is worth to mention that contributions of the O  $s$ -, Y  $s$ -, Y  $p$ -, V  $s$ - and V  $p$ -like states (not shown) are very minor throughout the conduction-band region. The second region of conduction band ranging from 7.2 eV for the zircon-type and 6.2 eV for the scheelite-type to higher values of energy is composed mainly of the Y  $4d$ -like states with slightly smaller contributions of the O  $2p$ -like states and a somewhat of the V  $3d$ -like states.

First-principles calculations reveal that in the two phases the O  $2p$ -like states dominate the upper part of the valence band and have significant contributions throughout the main portion of the valence band; however the V  $3d$ -like states contribute mainly near the bottom of the conduction band. It is necessary to mention that the linearized augmented plane wave (LAPW) calculations indicate that the minimum band gap of  $\text{YVO}_4$  is located at the  $\Gamma$  point at the center of the Brillouin zone, for both phases.

## Conclusions

We have investigated the structural properties and electronic properties of the zircon-type and the scheelite-type  $\text{YVO}_4$  using first-principles method. The calculated lattice parameters and the atomic positions of the zircon-type  $\text{YVO}_4$  are in good agreement with the experiment. The calculated phase transition pressure from the zircon-type structure to the scheelite-type structure is about 5.92 GPa, which compares well with the experimental value of 7.5 GPa. The calculated bulk modulus is 164 GPa for the zircon-type phase and 186 GPa for the scheelite-type phase. The scheelite-type phase bulk modulus is larger compared to that of the zircon-type phase and it reveals that the scheelite-type phase is more difficult to compress than the zircon-type phase. From the density of states and band structures, LAPW calculations indicate that the minimum band gap of  $\text{YVO}_4$  is located at the  $\Gamma$  point at the center of the Brillouin zone, for both phases. The use of the Engel–Vosko scheme has improved the results quite considerably; the calculated band gaps are 3.2 eV and

2.8 eV for zircon-type and the scheelite-type phase, respectively. We also conclude from this study that  $\text{YVO}_4$  is stable in the zircon-type phase. It is necessary to mention that in the two phases we found that the O  $2p$ -like states dominate the upper part of the valence band and have significant contributions throughout the main portion of the valence band; however the V  $3d$ -like states contribute mainly near the bottom of the conduction band, while Y atoms are lying far from the Fermi level.

*Acknowledgments.* One of the authors, S. Messekine would like to thank the University of Fribourg for awarding University Research Fellowship to carry out this work. This work is supported by the Swiss National Science Foundation.

## References

- [1] Jayaraman, A.; Kourouklis, G. A.; Espinosa, G. P.; Cooper, A. S. and Uiter, L. G. V.: A high-pressure Raman study of yttrium vanadate ( $\text{YVO}_4$ ) and the pressure-induced transition from the zircon-type to the scheelite-type structure. *J. Phys. Chem. Solids* **48** (1987) 755.
- [2] Terada, Y.; Shimamura, K.; Kochurikhin, V. V.; Barashov, L. V.; Ivanov, M. A. and Fukuda, T. J.: Growth and optical properties of  $\text{ErVO}_4$  and  $\text{LuVO}_4$  single crystals. *Crystal Growth* **167** (1996) 369.
- [3] O'Conner, J. R.: Unusual crystal-field energy levels and efficient laser properties of  $\text{YVO}_4$ :Nd. *Appl. Phys. Lett.* **9** (1966) 407.
- [4] Bagdasarov, Kh. S.; Kaminskii, A. A.; Krylov, V. S. and Popov, V. I.: Room-temperature induced emission of tetragonal  $\text{YVO}_4$  crystals containing  $\text{Nd}^{3+}$ . *Phys. Stat. Sol. (a)* **27** (1968) K1.
- [5] Kaminskii, A. A.; Bogomolova, G. A. and Li, L.: Absorption, fluorescence, stimulated emission and splitting of the  $\text{Nd}^{3+}$  levels in a  $\text{YVO}_4$  crystal. *Inorg. Mater. (USSR)* **5** (1969) 573.
- [6] Levine, A. K. and Palilla, F. C.: *Electrochem. Technol.* **4** (1966) 16.
- [7] Maunders, E. A. and DeShazer, L. G.: Use of yttrium orthovanadate for polarizers. *J. Opt. Soc. Am.* **61** (1971) 684.
- [8] Bernard, J. E. and Alcock, A. J.: High-efficiency diode-pumped Nd:YVO4 slab laser. *Opt. Lett.* **18** (1993) 968.
- [9] Bowkett, G. C.; Baxter, G. W.; Booth, D. J.; Taira, T.; Teranishi, H. and Kobayashi, T.: Single-mode 1.34 m Nd:YVO4 microchip laser with cw Ti:sapphire and diode-laser pumping. *Opt. Lett.* **19** (1994) 957.
- [10] Shen, D.; Liu, A.; Song, J. and Ueda, K.: Efficient operation of an intracavity-doubled Nd:YVO4/KTP laser end pumped by a high-brightness laser diode. *Appl. Opt.* **37** (1998) 7785.
- [11] Duclos, S. J.; Jayaraman, A.; Espinosa, G. P.; Cooper, A. S. and Maines, R. G. Sr.: Raman and optical absorption studies of the pressure-induced zircon to scheelite structure transformation in  $\text{TbVO}_4$  and  $\text{DyVO}_4$ . *J. Phys. Chem. Solids* **50** (1989) 769.
- [12] Long, Y. W.; Yang, L. X.; Yu, Y.; Li, F. Y.; Yu, R. C.; Liu, Y. L. and Jin, C. O.: High-pressure Raman scattering study on zircon to scheelite-type structural phase transitions of  $\text{RCrO}_4$ . *J. Appl. Phys.* **103** (2008) 093542.
- [13] Long, Y. W.; Zhang, W. W.; Yang, L. X.; Yu, Y.; Yu, R. C.; Ding, S.; Liu, Y. L. and Jin, C. Q.: Pressure-induced structural phase transition in  $\text{CaCrO}_4$ : Evidence from Raman scattering studies. *Appl. Phys. Lett.* **87** (2005) 181901.
- [14] Long, Y. W.; Yang, L. X.; You, S. J.; Yu, Y.; Yu, R. C.; Jin, C. Q. and Liu, J.: High-pressure Raman scattering and structural phase transition in  $\text{YCrO}_4$ . *J. Phys. Condens. Matter* **18** (2006) 2421.
- [15] Zhang, J.; Wang, J.; Zhang, H.; Wang, C.; Cong, H. and Deng, L.: First principles calculations of mechanical properties of the  $\text{YVO}_4$  single crystal. *J. Appl. Phys.* **102** (2007) 023516.
- [16] Dolgos, M. R.; Paraskos, A. M.; Stoltzfus, M. W.; Yarnell, S. C.; Woodward, P. M.: The electronic structures of vanadate salts: Cation substitution as a tool for band gap manipulation. *J. Solid State Chem.* **182** (7) (2009) 1964.
- [17] Stoltzfus, M. W.; Woodward, P. M.; Seshadri, R.; Klepeis, J.-H. and Bursten, B.: Structure and Bonding in  $\text{SnWO}_4$ ,  $\text{PbWO}_4$ , and  $\text{BiVO}_4$ : Lone Pairs vs Inert Pairs. *Inorg. Chem.* **46** (2007) 3839.

- [18] Zhi-Peng, C.; Yu-Hua, W. and Jia-Chi, Z.: A novel yellow emitting phosphor Dy<sup>3+</sup>, Bi<sup>3+</sup> co-doped YVO<sub>4</sub> potentially for white light emitting diodes. *Chinese Physics* **B19** (2010) 057803.
- [19] Kirschbaun, K.; Martin, A.; Parish, D. A. and Pinkerton, A. A.: Cooperative Jahn-Teller induced phase transition of TbVO<sub>4</sub>: single crystal structure analyses of the tetragonal high temperature phase and the twinned orthorhombic phase below 33 K. *J. Phys. Condens. Matter* **11** (1999) 4483.
- [20] Blaha, P.; Schwarz, K.; Sorantin, P. and Trickey, S. B.: Full-potential, linearized augmented plane wave programs for crystal-line systems. *Comput. Phys. Commun.* **59** (1990) 399.
- [21] Kohn, W. and Sham, L. J.: Self-consistent equations including exchange and correlation effects. *Phys. Rev.* **140** (1965) A1133.
- [22] Engel, E. and Vosko, S. H.: Exact exchange-only potentials and the virial relation as microscopic criteria for generalized gradient approximations. *Phys. Rev.* **B47** (1993) 13164.
- [23] Wang, X.; Loa, I.; Syassen, K.; Hanfland, M. and Ferrand, B.: Structural properties of the zircon- and scheelite-type phases of YVO<sub>4</sub> at high pressure. *Phys. Rev.* **B70** (2004) 064109.
- [24] Manjon, F. J.; Rodriguez-Hernandez, P.; Munoz, A.; Romero, H.; Errandonea, D. and Syassen, K.: Lattice dynamics of YVO<sub>4</sub> at high pressures. *Phys. Rev.* **B81** (2010) 075202.
- [25] Lehmann, G. and Taut, M.: On the Numerical Calculation of the Density of States and Related Properties. *Phys. Stat. Sol.* **B54** (1972) 469.
- [26] Kohanoff, J. and Gidopoulos, N. I.: Density functional theory: basics, new trends and applications. In: S. Wilson, Editor, *Handbook of Molecular Physics and Quantum Chemistry*, vol. 2, part 5, John Wiley & Sons Ltd., Chichester (2003), pp. 532–568 (Chapter 26).